Crosslinking and physical properties of poly (ethylene-*co*-vinyl acetate) produced by autoclave and tubular reactors

De Lemos Cristovao* and Robert Arnaud Roland Alain
Sahara International Petrochemical Company (SIPCHEM), Technology and Innovation Center (STIC, MANAR), Dhahran Techno Valley, Dhahran, Eastern Province, KINGDOM OF SAUDI ARABIA
*clemos@sipchem.com

Abstract

Four commercial poly (ethylene-co-vinyl acetate) grades, EVA, two produced by autoclave and two by tubular high-pressure reactors were selected to characterize the effect of molecular structure and long chain branching (LCB) onto the crosslinking performance, optical properties and thermal shrinkage of the converted films. HT-GPC and ^{13}C NMR spectroscopy techniques were used to determine the molecular structure and degree of LCB on EVA resins. Blends of EVA resin with organic peroxide, co-agent and antioxidant were prepared and converted into flexible foils.

The ordered comb-type structure of the tubular EVA showed lower molecular weight, narrower polydispersity index, lower degree of LCB and crystallinity degree at least 29 % higher when compared to autoclave EVA. It was assumed that the crosslinking kinetic is influenced by the ability of the radical species from the organic peroxides to easily abstract hydrogen from the terminal methyl groups of incorporated acetate units. Haze increases significantly with the presence of high content of LCB. Thermal shrinkage was found to be correspondent to the degree of LCB and inversely proportional to the degree of crystallinity.

Keywords: EVA, long chain branching, organic peroxide, crosslinking, autoclave, tubular.

Introduction

Photovoltaic (PV) modules based on crystalline solar cells for terrestrial applications are multilayer structures typically containing EVA films as the encapsulant material. Although various other alternative materials can be used, EVA is still by far the dominant encapsulation layer for PV modules accounting for nearly 80 % of the market.[10,11,15,22,28,30,35] EVA encapsulant sheets fulfill several basic functions to ensure long-term durability and the in-use performance of the PV modules. The outstanding properties of the EVA encapsulant sheets in PV systems can be attributed to several different functions that this material performs, all of which are key to the modules' assembly and proper functioning of the solar cell circuit over its full operational lifetime. These include easy handling and structural support, minimum optical transmission loss, withstanding long-term environment exposition, securing physical isolation and protection, maintaining reliable electrical isolation, limiting the ingression of moisture and oxygen and enhancing thermal conduction.[10,11,17,22,28,30,35]

EVA used to manufacture encapsulant film is a random ethylene/vinyl acetate copolymer (herewith denominated EVA or ethylene copolymer); for PV applications the vinyl acetate content is typically in the range 28 - 33% (w/w). The ethylene copolymer is either produced by a high pressure free radical initiated polymerization through continuous-flow mechanically stirred autoclave (vessel) or tubular polymerization technologies[18].

One of the major differences between both polymerization technologies is the operating pressure, which is set at 2,000 - 3,500 bar for tubular and at 1,100 - 2,000 bar for autoclave reactors[21]. Such difference creates reaction conditions that allows to obtain EVA resins with different degrees of branching[24,37]. Considering the process of producing EVA is the same as that used to produce LDPE, the long linear tubular reactor gives narrower molecular weight distribution and less long chain branching (LCB) type due to uniform residence time than the autoclave EVA resin.

On the other hand, the autoclave reactor produces ethylene copolymers with broader molecular weight distribution and more long chain branching[18]. Short chain branching (SCB) is present in both processes, but this type of species is not susceptible to hydrogen abstraction. The inductively destabilized radicals, that might eventually be formed[14], are not effective on increasing the rheological and final properties of the encapsulant film. Rudin et al[32] found that a LCB type has a minimum length of, at least, six carbon atoms.

To produce EVA encapsulant sheets, the pellets of the resin are typically blended with organic peroxides (that promote the crosslinking) and stabilizers and then converted into a flexible sheet. During the PV module lamination, the initially soft and translucent thermoplastic EVA-based foil is transformed into a highly transparent and thermo-mechanically stable material which limits its creep with time.[15,16,27] This so-called lamination process leads the EVA to crosslink into a three-dimensionally structure. This process triggers the creation of intermolecular chemical

**** Author for Correspondence***

links between the different nature of chains existent in the EVA.

During the heat-induced stage, the crosslinking agents are homolytically cleaved into radical species that scavenge hydrogen atoms from the polymers branch points, creating active radical sites[16].

Normally, the hydrogen withdrawal takes place from terminal methyl group of the incorporated acetate groups that creates crosslinking nets during PV modules lamination[25]. Thanks to the thermo-stability of the crosslinked EVA encapsulant sheet, the service life of the PV modules can reach 15 - 25 years.

Various investigations on the crosslinking mechanisms and the efficiency on the EVA-based encapsulation sheet have been published elsewhere[16,19,28]. In the field of the industrial application, there is still a gap on understanding the correlation between the molecular architecture of the EVA resins and the respective lamination performances of the encapsulant sheets produced. In this work, lab-scale EVA foils were manufactured using commercial EVA grades produced by autoclave and tubular reactors typically recommended for encapsulant sheets applications.

The aim is to correlate the molecular structures and branching degrees of the neat EVA resins with the crosslinking kinetic behavior and selected quality properties of the cured EVA foils. The outcomes from this investigation can help the encapsulant sheets manufacturers to optimize the formulations according to the lamination time requirements defined by the PV modules assemblers.

Material and Methods

Materials: Four commercial EVA resins were studied. The general properties are shown in table 1. The vinyl acetate (VA) contents of the EVA resins were determined using a Perkin Elmer Frontier bench-top FT IR spectrometry according to ASTM D 5594-18a. Melt flow index (MFI) characterizations were carried out on a Zwick Roell extrusion plastomer (model BMF-001) according to ASTM D 1238-13. The additive package with the respective concentrations blended with each EVA resin is shown in table 2.

Samples preparation: EVA pellets and the additives were mixed using an intensive mixer, Zeppelin Reimelt model FML4 (Henschel mixer) equipped with a mixing chamber (3 L net barrel volume) at room temperature and at a rotational speed of 250 rpm for a mixing time of 10 minutes. Typically, formulations using EVA encapsulant sheets for PV applications contain ultra-violet (UV) and light stabilizers and adhesion promoters (e.g. silane coupling agents) to warrant adhesion to glass and backsheet and long-term service work, respectively. Since the purpose of this work was to assess the crosslinking performance and selected physical properties over the different EVA resins, these raw materials were not included in the formulation.

The sheets of uncured EVA samples were produced using a OCS cast film extruder (L/D = 25/1) model ME 25/5800 V3. The following temperature setpoint were used to prepare the EVA sheets: 77/79/95/100/110 °C. Sheets measuring 500 ± 10 μm thicknesses were produced.

EVA films (area = 100 cm^2) were crosslinked by compression molding the uncured EVA foils in a Fontijne Grotnes press model LabEcon 600 at 150 °C under the pressure of 150 bar for a curing time of 7 min. The specimens prepared were used for crosslinking density, optical properties (haze and gloss) and thermal shrinkage characterizations. The samples were maintained in the same press for a cooling time of 5 min before releasing from the machine. The average thicknesses of the sheets were 270 ± 15 μm.

In the moving die rheometer (MDR) tests, 5 mm thickness molding sheets were made at 95 °C, 4.5 MPa at 6 min of pressing time. The samples were left in the compression molding machine for a cooling time of 3 min. 38 mm diameter discs were cut out from the molded sheets using punch press NAEF model B/36.

Table 1
General properties of the EVA commercial.

Ethylene copolymer	MFI, g/10min.	VA content, % (w/w)	Polymerization technology
EVA 1	13.7 ± 0.5	27.7 ± 0.1	Autoclave
EVA 2	17.8 ± 0.2	27.9 ± 0.1	Autoclave
EVA 3	23.2 ± 0.4	26.6 ± 0.2	Tubular
EVA 4	15.8 ± 0.3	26.8 ± 0.1	Tubular

Table 2
Additive package

Function	CAS No.	Commercial name	% (w/w)
Organic peroxide	34443-12-4	Luperox TBEC	0.39
Co-agent	1025-15-6	TAIC	0.79
Antioxidant	2082-79-3	Irganox 1076	0.010

Comprehensive characterizations were carried out using neat EVA resins, uncured and cured EVA sheets. NMR and HT-GPC characterizations were done using the EVA neat resins (pellets). Thermal analysis, micro compounder, MDR and optical properties experiments were performed using the uncured EVA films. Crosslinking density and thermal shrinkage were done using cured EVA foils.

High temperature gel permeation chromatography (HT-GPC): The molecular weights of the ethylene copolymers were determined relative to polystyrene standards in 1,2,4-trichlorobenzene solutions with sample concentrations 0.1 % (w/v) by HT-GPC using Viscotek-Malvern 350A pump at an elution rate of 1 mL/min at 150 °C. PLgel MiniMIX-B, 4.6 x 250 mm, 10 µm (Agilent Technologies) column recommended for high molecular weight polymers and differential refractive index (DRI) detector (Viscotek) were used in the experiments.

Nuclear Magnetic Resonance (NMR) Spectroscopy: EVA pellets (60 - 70 mg) were dissolved in 1,2,4-trichlorobenzene (0.4 mL) and a small amount (0.02 mL) of deuterated benzene was added as deuterium lock solvent. Gentle heating of the sample was necessary for complete dissolution.

NMR experiments were carried out at room temperature using Bruker Ascend™ 400 MHz wide bore magnet equipped with 5 mm liquids Broad Band probe (BBO) operating at 100.62 MHz for ^{13}C NMR. Pulse angle was set up at 9.8 µs, 20 s delay between each pulse (which is sufficient to allow complete relaxation of all carbon types in the sample) and a total of 4,096 scans. To be quantitative, no Nuclear Overhauser Effect (NOE) was not allowed which could bias signal enhancement for protonated carbons. Therefore, the decoupler mode was set to 'NNY'.

To simplify the ^{13}C NMR assignment, DEPT 135 (distortion-less enhancement by polarization transfer) was employed to assign carbon with odd number of protons attached i.e. -CH- and $-CH_3$ being positive and all $-CH_2-$ type being negative. To improve the signal-to-noise ratio in the ^{13}C NMR spectra, the Free Induction Decay (FID) was multiplied by 3 Hz line broadening factor. The chemical shifts of all the ^{13}C NMR spectra were referenced to the frequency of the $–CH_2–$ backbone resonating at 30.0 ppm, a common practice in polymer analysis[8,33].

Degree of LCB per 1000 carbons was calculated from the work carried out by Pooter et al[31] and ASTM D5017-17. equation 1 was used to determine the LCB per 1000 carbons.

$$\frac{LCB}{1000\ carbons} = \frac{1000\ x\ (mole\ \%\ alkyl\ branching)}{2\ x\ (mole\ ethene) + 6\ x\ (mole\ \%\ alkyl\ branching)} \quad (1)$$

Differential Scanning Calorimetry (DSC): Thermal behavior was analyzed by differential scanning calorimetry using a Perkin Elmer DSC 8500 under 50 mL/min nitrogen flow. The instrument was calibrated with indium. Uncured EVA film samples (5 ± 1 mg) were melted at 100 °C (to avoid premature organic peroxide decomposition), held at this temperature for 5 min, to ensure complete melting, cooled to 10 °C and heated up again to 150 °C. All heating and cooling rates were performed at 10 °C/min. The melting temperature (T_m) and enthalpy of fusion ($\triangle H_f$) were taken from the second heating curve. Crystallinity degree (X_c) was calculated according to equation 2.

$$X_c = \frac{\Delta H_f}{\Delta H_f^*}\ x\ 100\ \% \quad (2)$$

where ΔH_f^* is the enthalpy of fusion of the perfect polyethylene (PE) crystal and ΔH_f is the enthalpy of fusion of the four EVA samples respectively. The value of ΔH_f^* for PE is 277.1 J/g[4].

Crosslinking density: Crosslinking density was determined by solvent extraction according to ASTM D 2765-16. Samples weighing about 1 g were cut from different sections of each cured EVA sheet and put into a glass bottle containing 100 mL of xylene. The exact initial weight of each sample (m_0) was determined on a precision balance. The apparatus was placed inside an oven at 110 °C for 12 h.

After completing the extraction, the insoluble residues were dried at 110 °C for 8 h followed by determination of the net weights (m). The gel percentage, which it is directly related to crosslinking density, was calculated according to equation 3.

$$Crosslinking\ density = \frac{m}{m_0}\ x\ 100\ \% \quad (3)$$

Micro compounder: The crosslinking kinetics of the EVA blends were investigated by using a DSM Xplore melt compounder (model 2009), which has 0.015 L net barrel capacity volume, using twin screw speed of 100 rpm with barrel temperature set at 120 °C.

Moving die rheometer (MDR): The crosslinking onset (t_1), kinetics of crosslinking reaction time (t_{90}) and dynamics torques, (M_H and M_L) of the EVA compounds were measured by the moving die rheometer (Model 2000 from Alpha Technologies) at 120 °C and 60 min.

As reported by Thaworn et al[35], the cure rate index (CRI) can be estimated using equation 4.

$$CRI = \frac{100}{t_{90} - t_1} \quad (4)$$

Optical properties - haze and gloss 45°: Haze measurements were carried out on a Hazemet Gamma 12 model OHM-V2 made Optical Control Systems, according to ASTM D1003-13. Gloss measurements were carried out on a Micro Gloss 60° made by BYK-Gardner, using light source C, according to ASTM D2457-13. Haze and gloss were measured using uncured EVA sheets.

Thermal shrinkage: Thermal shrinkage of crosslinked EVA sheets was determined by measuring the largest horizontal shrinkage after 5 min at 110 °C on a glass plate.

Results and Discussion

Molecular structure and thermal behavior: High temperature gel permeation chromatography (HT-GPC) analysis was carried out in order to determine the molecular weights and molecular weight distribution of the four EVA resins. As reported by Folie et al[14], HT-GPC-DRI is a good technique to estimate the number average molecular weight (M_n), weight average molecular weight (M_w) and polydispersity index (PDI) of ethylene copolymers. The characteristics curves and the properties of the four ethylene copolymers are shown in figure 1 and table 3 respectively.

EVA 1 and 2 and EVA 3 and 4 showed similar M_n indicating similar colligative properties. Higher M_w and M_z properties were observed for the EVA resins produced by autoclave reactor. Therefore, higher polydispersity indexes were noticed for EVA resins obtained by the continuous-flow mechanically stirred autoclave reactor. These findings confirm what have been published elsewhere[23,29,25].

In the tubular reactor the mass is transported as a plug flow and the cooling takes place by the cold water circulating around the tube. The laminar flow throughout the reactor is uniform, so that the residence time of each polymeric unit is approximately the same, leading to narrower molecular weight distribution with less LCB[26]. On the other hand, in the autoclave reactor the one-phase polymer/gas medium meets periodical feeds of fresh and cold ethylene, creating different residence times for each polymer chain. Such reaction medium contributes to broader molecular weight distribution, higher molecular weights and LCB formation which is, eventually, evidenced by the molecular shoulder at the GPC curve[29].

Although Folie et al[14] describe that M_w values from HT-GPC-DRI do not consider the contributions of the molecular weights of the branching, the results clearly showed two distinguished clusters. The findings reveal EVA 1 and 2 with highest M_w against EVA 3 and 4 showing lower M_w values.

NMR spectroscopy was employed for determining the branching degree in the ethylene copolymers through the detection of the frequency shifts for carbon atoms at branch points by high frequency ^{13}C NMR using DEPT 135 method. The mechanism of LCB formation is not well established yet, but the most accepted explanation is the random intermolecular reaction even though in some cases this mechanism does not explain the phenomenon observed[22,37]. Branching with six or more carbon atoms is considered as LCB[17,32] and these branches effectively participate in the crosslinking mechanism.

Representative ^{13}C-NMR spectra of the four ethylene copolymers are given in figure 2. A single peak at 169.58 ppm pertaining to acetoxy carbonyl carbon of the vinyl acetate unit has been found and it is not included in the calculation. The most intricate region of the ^{13}C NMR spectra is the 0-75 ppm chemical shift range which, indeed, is the typical range used to differentiate the LCB degrees among the EVA resins. Assignments were done according to the work carried out by Beshah[3] and the chemical shifts are presented in table 4.

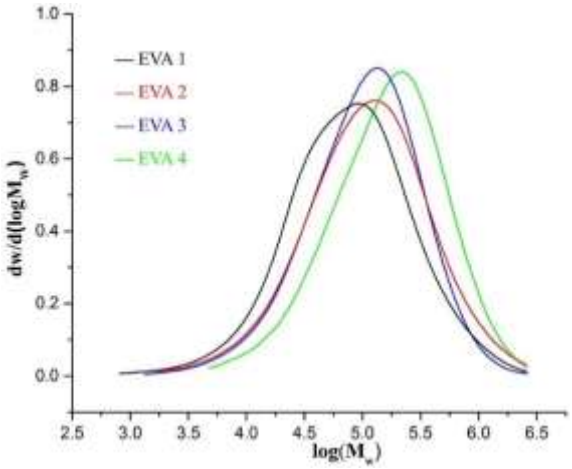

Figure 1: HT-GPC-DRI curves of EVA resins.

Table 3
Molecular characteristics of EVA samples.

Sample	M_n (kg/mol)	M_w (kg/mol)	M_z (kg/mol)	PDI
EVA 1	33.2	158.9	534.1	4.78
EVA 2	32.8	151.1	535.2	4.62
EVA 3	29.1	108.9	274.7	3.74
EVA 4	29.6	104.2	326.6	3.52

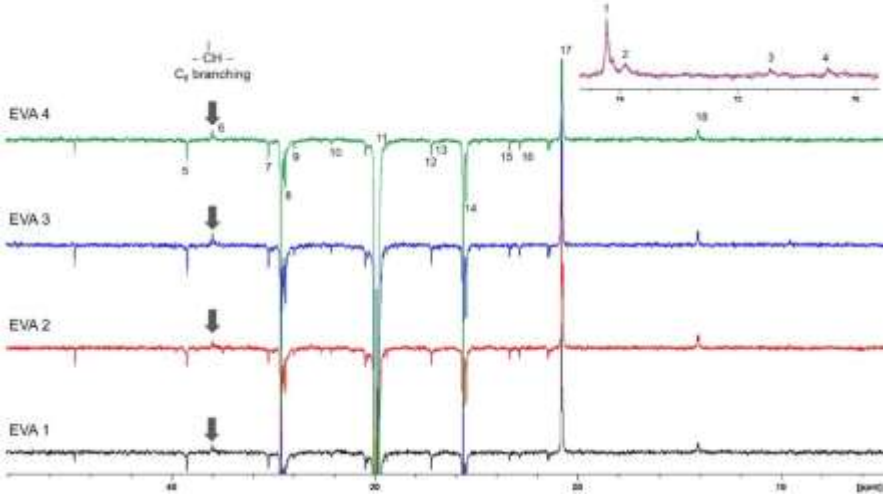

Figure 2: ^{13}C NMR spectra for EVA resins.

Table 4
Chemical shifts typically observed for ethylene copolymers with the corresponding carbon and sequence assignments.

Chemical shift (ppm)	Carbon assignment	Sequence assignment
169.58	C=O	(VA)
74.23	Tδδ+ branch CH	EVE
73.90	Tδδ+ branch CH	EEV/VEV
71.41	Tβδ+ branch CH	VVE
70.47	Tββ branch CH	VVV
39.27	Sαδ+ CH_2	VVE
38.05	CH	C_6 branch
35.26	Sαα CH_2	VVV
34.62	Sαδ+ CH_2	EVE
34.39	CH_2	3S end group
32.13	CH_2	EEE
30.00	CH_2 backbone	EEE
27.21	CH_2	EEE
26.82	Sβδ CH_2	VVE
25.58	Sβδ CH_2	EVE
23.39	Sββ CH_2	VEV
22.85	CH_2	2S end group
20.84	CH_3	(VA)
14.11	CH_3	C_6 -CH_3 & 1S end group

E = ethylene unit; V = vinyl acetate unit

Table 5
LCB results of the EVA resins.

Sample	EVA 1	EVA 2	EVA 3	EVA 4
LCB/1000 carbons	7.6	9.6	5.3	6.8

The branching characteristic of the LCB chemical shift is present for the four EVA resins. Branches with more than six carbon atoms were not differentiated due to the limitation of the technique. The degree of LCB per 1000 carbons was calculated according to equation 1 and the results are shown in table 5. The trend towards higher level of LCB for autoclave EVA and lower values for EVA produced by tubular technology is clear. Thermal properties of uncured EVA films were measured. As previously indicated, the ethylene copolymer resins were subjected to a thermal pretreatment prior to examination by DSC, to establish comparable thermal histories for all the samples.

Table 6 reveals that autoclave ethylene copolymers show lower melting and crystallization temperatures as well as lower crystallinity degree when compared to EVA 3 and 4. It is suggested that the highest VA contents values for EVA 1 and 2 is one of the factors that contribute to decrease the crystallinity degree of the autoclave EVA resins. Shi et al[34] describe that the variabilities in the degree of on crystallinity

in the EVA resins are explained by the intra-molecular defects created by the pendent acetoxy group. Thereby, the likelihood of differences in the distribution and sequence of the pendant acetoxy groups in the polymer chain is reasonable, which also affects the thermal properties of the EVA resins. Coutinho et al[9] reported that the higher the degree of crystallinity degree, the higher is the chain packing.

Crosslinking behavior: Luperox L-TBEC is a peroxyester crosslinking agent that belongs to the monoperoxycarbonate peroxide's family. Luperox L-TBEC generates high-energy free radicals that provide both efficient and faster crosslinking of EVA encapsulant sheets creating high energy radicals of 439.5 kJ/mol[2]. According to Thaworn et al[35], organic peroxides which generate free radicals $\geq$ 418.6 kJ/mol show high crosslinking efficiency due to the ability of the radical species to easily scavenge hydrogen present in most potential crosslinkable polymers[7,14].

TAIC is a co-agent which is highly reactive towards free radicals[13]. It is a reactive raw material which boosts the Luperox L-TBEC efficiency by suppressing inefficient side reactions, like chain scission and disproportionation[1,5,18]. TAIC is classified as type II co-agent and its use leads to an increase in crosslinking density of the EVA sheet during the lamination process.

In the micro compounder equipment, the crosslinking behavior of the four EVA materials is isothermally evaluated. The kinetics curves in figure 3 show the following trend in terms of crosslinking speed: EVA 1 > EVA 2 > EVA 4 > EVA 3. At the first 2 min of the experiment, the melting stage of the EVA resins is initiated. At about the same period, the organic peroxide and co-agent begin the cleavage process in radical species. During this time, it is inferred that few effective crosslinking reactions might take place. In the micro compounder, the torque data were collected at 0.1 min (6 s) time intervals.

Considering the shear effect and the reactive conditions during the experiments, the technique is suitable to infer the crosslinking kinetic profile of the four different systems. More accurate onset of crosslinking reaction and the minimum and maximum torque values were obtained through moving die rheometer (MDR).

Equations 5 to 8 were derived from empirical fitting the kinetic curves shown in figure 3 within the reaction time from 2 to 9.5 min. The estimated R^2 values show the mathematical models goodness-of-fit and explain the response variable.

EVA 1 $Torque = 62.242\ t^2 - 543.77\ t + 7275.9$
$R^2 = 0.9944$ (5)

EVA 2 $Torque = 35.871\ t^2 - 331.76\ t + 5780.7$
$R^2 = 0.9785$ (6)

EVA 3 $Torque = 2.771\ t^2 - 23.353\ t + 4677.2$
$R^2 = 0.9926$ (7)

Table 6
Thermal properties of neat EVA.

Sample	T_m (°C)	T_c (°C)	$\triangle H_f$ (J/g)	X_c (%)
EVA 1	71.2	50.3	21.5	7.8
EVA 2	71.6	49.8	24.4	8.8
EVA 3	74.7	52.1	31.6	11.4
EVA 4	73.8	51.9	34.7	12.5

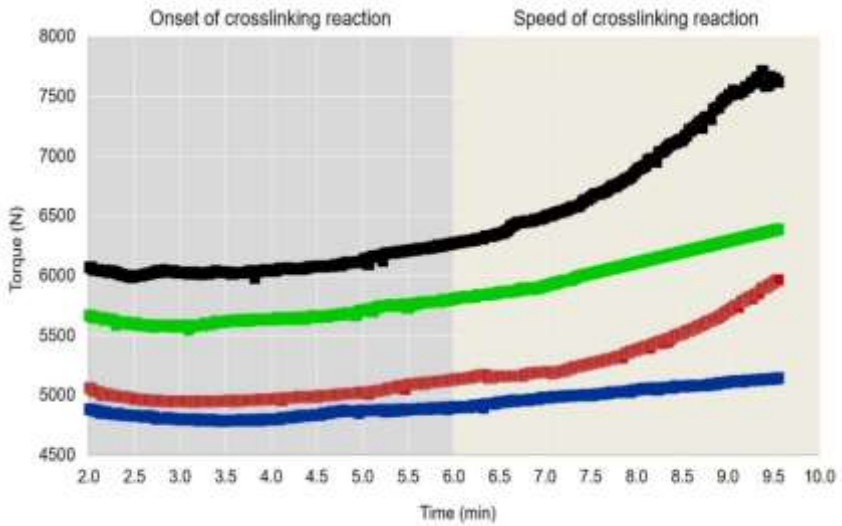

Figure 3: Crosslinking kinetics of the EVA compounds (■) EVA 1, (■) EVA 2, (■) EVA 3 and (■) EVA 4.

EVA 4 $Torque = 14.745\ t^2 - 59.872\ t + 5637.0$
$R^2 = 0.9978$ (8)

The speed of reaction can also be inferred from the slope of the derivative of equations 5 to 8. Thereby, it is confirmed the following sequence with respect to the crosslinking speed: EVA 1 > EVA 2 > EVA 4 > EVA 3.

Once the crosslinking reaction is set off, the radical species trigger off propagation reactions by abstracting hydrogen from the vinyl acetates branches. The chemical bonds subsequently created shift the thermoplastic characteristic of the EVA sheet into a thermoset and durable material[30]. In the figure 3, it is noticed that EVA 1 and 2 show the fastest speed of crosslinking kinetics due to the respective highest curve steepness after 6 min of reaction. Since EVA produced by tubular reactor is more comb-type[6] and show evidences of subtle higher X_c, it is suggested that a more ordered, well-orientated and folded structure ethylene copolymer is produced.

Therefore, one believes that the abstraction of hydrogen from the terminal methyl groups of incorporated acetate groups by the radical species is more difficult due to the lower number of LCB and well-packed configuration of the chains. On the other hand, considering the higher number of LCB in autoclave EVA, the accessibility to the methyl group is easier, enabling the reactive species to abstract hydrogen and make chemical bonds more effectively. Thus, the active species from organic peroxide are consumed faster after the EVA resin is melted triggering off several crosslinking reactions between the terminal groups of the long-chain branches. Hence, torque is increased and the flexible encapsulant sheet is converted into a transparent and thermomechanical stable material.

Results from MDR show higher values of torque (M_H) for EVA 1 and 2 sheets suggesting that more crosslinking reactions takes place and hence, the viscosity is increased (Table 7). The findings reveal as well that t_1 results of EVA 3 and 4 are 39.33 and 38.23 min respectively confirming the slowest onsets of curing for tubular EVA-based encapsulant sheets.

Contrarily, EVA 1 and 2 revealed fastest onset of crosslinking reaction, considering t_1 results are < 30 min. As expected, the four EVA foils show similar optimum curing time (t_{90}) and the results depend on the half-life time of the organic peroxide.

According to product datasheet[2], at 120.9 °C the half-life time of Luperox L-TBEC is 60 min. Although MDR experiments were set up to 60 min, it was noticed that the maximum torques (M_H) values were reached after 41 - 43 min. The difference between maximum and minimum torques (M_H - M_L) is important to assess viscosity increasing after completing the crosslinking reactions. Higher values of M_H - M_L were observed for EVA 1 and 2. In an industrial application, this could lead to longer service life for those encapsulant sheets manufactured using EVA 1 and 2 resins.

Figure 4 shows the comparative analyses between CRI, calculated as per the equation 4 and steady-state torque, calculated at 6, 7, 8 and 9 min using equations 5 to 8. It is pointed out that CRI reflects the time for the crosslinking reaction occurs and complements M_H - M_L results. EVA 3 and 4 show the higher CRI values while EVA 1 and 2 exhibit the lower CRI. The lower are the CRI values, the longer is the time for the radical species to scavenge the hydrogen atoms from the branches.

Therefore, more crosslinking reactions between chains occur and, consequently, the higher is the viscosity. As shown in the histogram plots in figure 4, the viscosity of autoclave EVA 1 and 2 respectively, increases by 19 and 12 %. On the other hand, tubular EVA foils showed the viscosity of EVA 3 and 4 raises by 8 and 4 % respectively.

The degree of crosslinking in EVA-based encapsulant sheets is normally expressed as a percentage of gel content. It depicts an indication of the polymer fraction that is not extractable with an organic solvent. In industrial production lines, the EVA foil is subjected to gel content determination to confirm crosslinked fraction before undergoing the lamination process. The results are meaningful to confirm the performance of the EVA sheet, which is typically part of the film technical specification.

Results from table 7 show higher amount of gel content for encapsulant sheets manufactured using autoclave EVA resins. Average crosslinking density of EVA 1 and 2 is respectively 89.2 and 87.1 %. Thereby, the crosslinking density results confirm the hypothesis of easier hydrogen abstraction from autoclave EVA which contains higher degree of LCB.

Table 7
MDR and gel content results.

Sample	t_1 (min)	t_{90} (min)	M_L (lbf-in)	M_H (lbf-in)	M_H - M_L	Gel content (%)
EVA 1	28.59 ± 0.03	42.85 ± 0.05	0.31 ± 0.01	3.36 ± 0.01	3.05 ± 0.01	89.1 ± 0.4
EVA 2	29.89 ± 0.03	42.56 ± 0.03	0.26 ± 0.01	2.58 ± 0.01	2.32 ± 0.01	87.2 ± 1.3
EVA 3	39.33 ± 0.03	42.92 ± 0.04	0.20 ± 0.01	1.55 ± 0.01	1.35 ± 0.01	84.7 ± 1.1
EVA 4	38.23 ± 0.03	41.93 ± 0.04	0.29 ± 0.01	1.72 ± 0.01	1.43 ± 0.01	83.5 ± 0.3

Xia et al[36] showed that crosslinking enhances the thermomechanical properties of EVA and this limits its creep with time. On the other hand, an insufficient degree of crosslinking might lead to creep at the bounds of the working temperature of the PV module.

Thaworn et al[35] observed that the torque difference between M_H - M_L can, directly, relate to gel content measured on EVA foils prepared using different crosslinking temperatures. Extrapolating this finding, it was noticed that in a same crosslinking temperature and time, a good correlation between M_H - M_L and gel content is figured out (Figure 5).

The monitoring of the crosslinking efficiency of the EVA-based encapsulant sheets by using MDR brings several benefits. Apart from the cost reductions initiatives, like less organic solvent consumption and expenses related to a proper residue disposal, MDR experiments allow trimming the time to obtain the lab result.

Optical properties: Optical properties of the EVA encapsulant sheets, which refer to haze and gloss, are controlled by the degree of LCB[20]. There are other relevant factors to be considered in haze and gloss properties as well: degree of crystallization, crystal structure, crystal size and relaxation time of polymers. It is known that LCB increases relaxation time of polymers[26]. At higher relaxation time, the crystallization occurs under influence of stress elongation; hence, lower crystallinity degree and less oriented crystalline structures are observed.

On the other hand, the well oriented crystalline structures allow the polymeric chains accommodated easier, hence, decrease the surface roughness.

EVA foils manufactured using tubular EVA resin showed lower haze values and higher gloss results as shown in figure 6. Previously, the findings from ^{13}C NMR (Table 5) confirmed the trend towards lower degree of LCB/1000 C for tubular EVA resin. The difference in gloss results comparing either the two autoclave EVA resins or the two tubular EVA resins is minimum. Nonetheless, there are clear differences in gloss and haze properties being suggested that such differences depend on the polymerization technology.

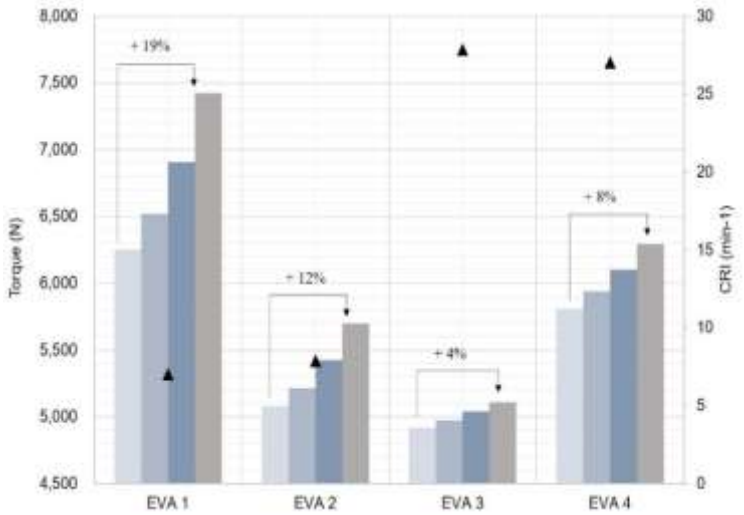

Figure 4: Correlation between CRI (▲) and torque at (■) 6 min; (■) 7 min; (■) 8 min; (■) 9 min.

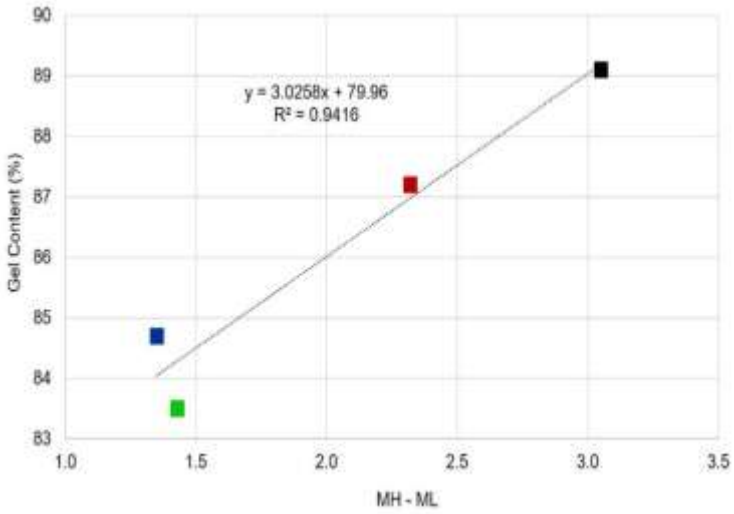

Figure 5: Correlation between torque difference and gel content (■) EVA 1, (■) EVA 2, (■) EVA 3 and (■) EVA 4.

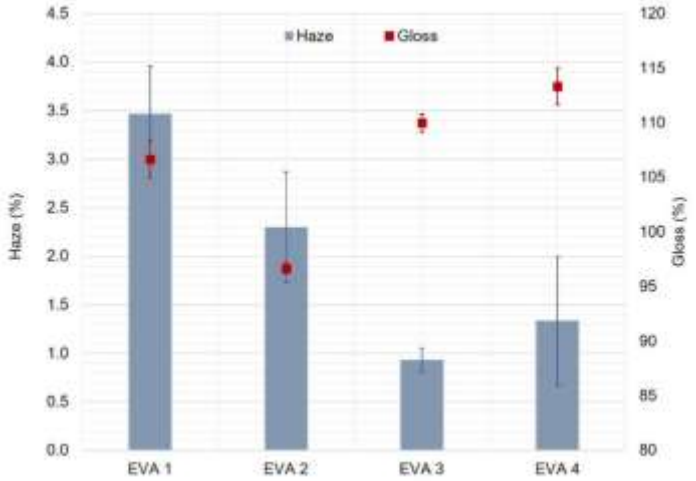

Figure 6: Haze and gloss results of the EVA compounds

Table 8
Thermal shrinkage results.

Sample	EVA 1	EVA 2	EVA 3	EVA 4
Thermal shrinkage (%)	2.3 ± 0.2	2.7 ± 0.3	1.0 ± 0.2	1.7 ± 0.1

Thermal shrinkage: Thermal shrinkage is one of the key quality properties and generally caused due to process induced stress during the manufacturing of the EVA foils. The EVA encapsulant sheet is prone to shrinkage mainly due to the macromolecular chain orientation in the casting forming process. The PV modules manufacturers define certain limits of thermal shrinkage depending on the environment wherein the PV cell will be installed. Thermal shrinkage results of the four EVA encapsulant sheets are shown in table 8. Higher values are observed for the foils produced using autoclave EVA (EVA 1 and 2) in contrast to EVA 3 and 4 which showed the lowest results. When extruding the EVA foil, the anisotropic expansion is the key to control the shrinkage performance[12,23].

Normally, in machine direction, the polymer molecules get aligned and remain oriented due to the fast cooling process. The more crystalline nature of EVA 3 and 4 gives less chains mobilities so that lower thermal shrinkage is observed. On the other hand, EVA 1 and 2 showed lower values of crystallinity degree and thus, the relaxation of orientations is more pronounced. Thermal shrinkage always requires special attention since it can give rise to quality issues like microcracks defects leading to reduced efficiency and a shortened life span[13,26] or, in latest practice in industry, scrap the entire PV module. One of the possibilities to reduce the thermal shrinkage is to reduce the extrusion output and the speed of the relaxing roll. The technical datasheets from different EVA foils producers across the Globe show thermal shrinkage data lower than 5 % or even less as desirable.

Conclusion

Commercial EVA resins produced by autoclave and tubular reactors were blended with crosslinking additives and converted into crosslinked EVA foils. The microstructure of the EVA neat resin was found to affect the crosslinking behavior and quality properties of the encapsulant sheet. Differences in molecular weights between autoclave and tubular EVA resins were confirmed. Degree of LCB showed a trend towards higher number of LCBs per 1000 carbons in the autoclave EVA resins. Thermal properties of the tubular EVA resins revealed higher crystallinity degrees.

The lower degree of LCB on the EVA tubular resins resulted in slower crosslinking kinetics, lower gel content and lower torque increase. This study showed evidence that the more ordered comb-type structure of the tubular EVA hampers the abstraction of hydrogen from the well-packed terminal methyl groups of incorporated acetate groups by the radical species. For a same crosslinking formulation, the autoclave EVA resin showed higher torque increase.

Hence the greater the degree of crosslinking between the branches, the better the thermo mechanical stability of the entire encapsulant sheet. In the field of the application, this work showed the possibility of using results of M_H - M_L to predict the gel content of the crosslinked a EVA foil reducing significantly the time of analysis, organic solvent consumption and residues disposal.

Regarding optical properties, it was confirmed the films produced by tubular ethylene copolymer resins result in lower haze and higher gloss properties. These parameters depend on the degree of crystallinity, LCB and orientation of the crystals.

Thermal shrinkage results revealed that the higher is the crystalline nature, the lower is the chain mobility and the lower is the film contraction.

Acknowledgement

The authors are thankful to Dr. Nikolaos Hadjichristidis from King Abdullah University of Science and Technology (KAUST) for his experimental assistance on the HT-GPC analyses. This work was supported by SIPCHEM and the authors would like to express their gratitude to the Company.

References

1. Akzo Nobel Co., Application of coagents for peroxide crosslinking Technical Bulletin, http://www.neochemical.ru/File/Brochure%20crosslinking%20peroxides.pdf, Accessed March 23rd **(2020)**

2. Arkema Inc., Product Bulletin, Luperox TBEC Organic Peroxide: Technical Information, https://intranet.ssp.ulaval.ca/cgpc/fsss/fichiers/luperox-tbec_tech.pdf, Accessed April 17th **(2020)**

3. Beshah K., Microstructural analysis of ethylene-vinyl acetate copolymer by 2D NMR spectroscopy, *Macromolecules*, **25(21)**, 5597-5600 **(1992)**

4. Brandrup J., Immergut E.H. and Grulke E.A., Polymer Handbook, 4th ed., Wiley-Inter Science Publishing, New York, USA **(1999)**

5. Bucsi A. and Szocs F., Kinetics of radical generation in PVC with dibenzoyl peroxide utilizing high-pressure technique, *Macromol. Chem. Phys.*, **201**, 435-438 **(2000)**

6. Butler T.I. and Morris B.A., PE-Based Multilayer Film Structures, Plastic Films in Food Packaging, materials, technology and applications, New York, USA, Elsevier, 21-52 **(2013)**

7. Callais P.A., Organic Peroxides, In Tracton A., ed., Coating Technology Handbook, 3rd ed., CRC Press, Boca Raton, Florida, USA **(2006)**

8. Charlier Q., Girara E., Freyermouth F., Vandesteene M., Jacquel N., Ladavière C., Rouseau A. and Fenouillot F., Solution viscosity – molar mass relationships for poly(butylene succinate) and discussion on molar mass analysis, *Express Polym. Lett.*, **9(5)**, 424-434 **(2015)**

9. Coutinho F.M.B., Mello I.L. and Santa Maria L.C., Polietileno: Principais Tipos, Propriedades e Aplicações, *Polímeros*, **13(1)**, 1-13 **(2003)**

10. Cuddihy E.F., Burger D.R., Willis P., Baum B., Garcia A. and Minning C., Polymer Encapsulation Materials for Low-Cost Terrestrial Photovoltaic Modules, In Geblein C.G., Williams D.J. and Deanin R.D., eds., Polym. Sol. Ener. Utilization, American Chemical Society, 353-366 **(1983)**

11. Czanderna A.W. and Pern F.J., Encapsulation of PV Modules Using Ethylene Vinyl Acetate Copolymer as a Pottant: A Critical Review, *Sol. Energ. Mat. Sol. C.*, **43**, 101-181 **(1996)**

12. Dartora P.C., Santana R.M.C. and Moreira A.C.F., The influence of long chain branches of LLDPE on processability and physical properties, *Polímeros*, **25(6)**, 531-539 **(2015)**

13. Dluzneski P.R., Peroxide Vulcanization of Elastomers, *Rubber Chem. Technol.*, **74(3)**, 451-492 **(2001)**

14. Folie B., Kelchtermans M., Shutt J.R., Schonemann H. and Krukonis V., Fractionation of poly(ethylene-co-vinyl acetate) in supercritical propylene: towards a molecular understanding of a complex macromolecule, *J. Appl. Polym. Sci.*, **64**, 2015-2030 **(1997)**

15. Hirschl Ch., Neumaier L., Puchberger S., Mühleisen W., Oreski G., Eder G.C., Frank R., Tranitz M., Schoppa M., Wendt M., Bogdanski N., Plösch A. and Kraft M., In-line determination of the degree of crosslinking of ethylene vinyl acetate in PV modules by Raman spectroscopy, *Sol. Energ. Mat. Sol. C.*, **152**, 10-20 **(2016)**

16. Hirschl Ch., Neumaier L., Puchberger S., Mühleisen W., Oreski G., Eder G., Frank R., Tranitz M., Schoppa M., Wendt M., Bogdanski N., Plösch A. and Kraft M., Determination of the degree of ethylene vinyl acetate crosslinking via Soxhlet extraction: Gold standard or pitfall?, *Sol. Energ. Mat. Sol. C*, **143**, 494-502 **(2015)**

17. Hou L., Fan G., Guo M., Hsieh E. and Qiao J., An improved method for distinguishing branches longer than six carbons (B_{6+}) in polyethylene by solution ^{13}C NMR, *Polymer*, **53(20)**, 4329-4332 **(2012)**

18. Knuuttila H., Lehtinen A. and Nummila-Pakarinen A., Advanced Polyethylene Technologies - Controlled Material Properties, *Adv. Pol. Sci.*, **169**, 29-73 **(2004)**

19. Li H.Y., Théron R., Röder G., Turlings T., Luo Y., Lange R.F.M., Ballif C. and Perret-Aebi L.E., Insights into the encapsulation process of photovoltaic modules: GCMS analysis on the curing step of Poly(ethylene-co-vinyl acetate) (EVA) encapsulant, *Polym. Polym. Comp.*, **20(8)**, 665-672 **(2012)**

20. Lignell D., Possibilities of autoclave LDPE process, Degree Thesis Plastteknik, Arcada, 8-30 **(2015)**

21. Malpass D.B., An overview of Industrial Polyethylene: Properties, Catalysts and Processes, Wiley-Scrivener Publishing LLC **(2010)**

22. McDaniel M.P., Rohlfing D.C. and Benham E.A., Long Chain Branching in Polyethylene from the Phillips Chromium Catalyst, *Polym. React. Eng*, **11(2)**, 101-132 **(2003)**

23. Meyer S., Timmel S., Braun U. and Hagendorf C., Polymer Foil Additives Trigger the Formation of Snail Trails in Photovoltaic Modules, *Energy Procedia*, **55**, 494-497 **(2014)**

24. Nexant, Poly Olefins Global Technology Analysis, POPS Program, Section 2:2-1-2-43 **(2016)**

25. Nijhof E., Relationship Rheological Behavior and Molecular Architecture of LDPE's Designed for Extrusion Coating, Proceedings of the 11th TAPPI European Place Conference, Athens, Greece, 1554-1578 **(2007)**

26. Nippe T., Schaarshmidt H. and Poltersdorf B., EVA Sheet - A High-End Product, Kunststoffe International 4/2012, 41-43 **(2012)**

27. Ogier S., Vidal C., Chapron D., Bourson P., Royaud I., Poncot M., Vite M. and Hidalgo M., A comparative study of calorimetric methods to determine the crosslinking degree of the ethylene-co-

vinyl acetate polymer used as a photovoltaic encapsulant, *J. Polym. Sci. Part B: Pol. Phys.*, **55**, 866-876 **(2017)**

28. Oliveira M.C.C. de, Cardoso A.S.A.D., Viana M.M. and Lins V.F.C., The causes and effects of degradation of encapsulant ethylene vinyl acetate copolymer (EVA) in crystalline silicon photovoltaic modules: A review, *Renew Sust. Energ. Rev.*, **81(2)**, 2299-2317 **(2018)**

29. Peacock A.J., Handbook of polyethylene: structures, properties and applications, Marcel Dekker, New York, USA, 43-53 **(2000)**

30. Peike C., Purschke L., Weiss K.A., Köhl M. and Kempe M., Towards the origin of photochemical EVA discoloration, In Proceedings of the PVSC 39th IEEE photovoltaic specialist conference (PVSC 39), IEEE-PVSC, Tampa, Florida, USA, 1579-1584 **(2013)**

31. Pooter M., Smith P., Dohrer K., Bennett K., Meadows M., Smith C., Schouwenaars H. and Geerards R., Determination of the composition of common linear low-density polyethylene copolymers by ^{13}C-NMR spectroscopy, *J. Appl. Polym. Sci*., **42**, 399-408 **(1991)**

32. Rudin A., Grinshpun V. and O'Driscoll K.F., Long Chain Branching in Polyethylene, *J. Liq. Chrom.*, **7**, 1809-1821 **(1984)**

33. Samperi F., Montaudo M., Puglisi C., Alicata R. and Montaudo G., Essential role of chain ends in the Ny6/PBT exchange. A combined NMR and MALDI approach, *Macromolecules*, **36**, 7143-7154 **(2013)**

34. Shi X.M., Zhang J., Jin J. and Chen S.J., Non-isothermal crystallization and melting of ethylene-vinyl acetate copolymers with different vinyl acetate contents, *Eexpress Polym. Lett.*, **2(9)**, 623-629 **(2008)**

35. Thaworn K., Buahom P. and Areerat S., Effects of Organic Peroxides on the Curing Behavior of EVA Encapsulant Resin, *Open J. Polym. Chem.*, **2(2)**, 77-85 **(2012)**

36. Xia Z., Cunningham D. and Wohlgemuth J., A new method for measuring cross-link density in ethylene vinyl acetate-based encapsulant, *Photovolt. Int*., **5**, 150-159 **(2009)**

37. Yang Q., Jensen M.D. and McDaniel M.P., Alternative View of Long Chain Branch Formation by Metallocene Catalysts, *Macromolecules*, **43(21)**, 8836-8853 **(2010)**.

(Received 14th May 2020, accepted 12th July 2020)